MULTI-FIELD STABILIZED FINITE ELEMENT APPROXIMATIONS FOR OLDROYD-B FLUID FLOWS

D. D. dos Santos [a], S. Frey [b], M. F. Naccache[c], and P. R. de Souza Mendes[d]

[a,b] Universidade Federal do Rio Grande do Sul
Department of Mechanical Engineering
Porto Alegre, RS 90050-170, Brasil
[a] dallonder@mecanica.ufrgs.br
[b] frey@mecanica.ufrgs.br
[c,d] Pontifícia Universidade Católica do Rio de Janeiro
Department of Mechanical Engineering
Rio de Janeiro, RJ 22453-900, Brasil
[c] naccache@puc-rio.br
[d] pmendes@puc-rio.br

Received: November 28, 2012
Revised: December 29, 2012
Accepted: January 29, 2013

ABSTRACT

This work concerns with numerical simulations of creeping and inertial flows of viscoelastic fluids. The mechanical model consists of mass and momentum balance equations, coupled with the Oldroyd-B fluid. The model is approximated by a multi-field Galerkin least-squares (GLS) methodology in terms of extra-stress, velocity and pressure. The GLS method, introduced by Hughes et al. (1986) in the context of the Stokes problem for Newtonian fluid flows, allows the use of combinations of equal-order finite element interpolations and remains stable even for elastic- and inertia-dominated fluid flows. Some steady simulations of Oldroyd-B fluids, flowing over a slot, are herein carried out. The influence of inertia and fluid viscoelasticity is taken into account ranging the Reynolds and Weissenberg numbers for relevant values of this flow. The results are in accordance to the viscoelastic literature and reassure the fine stability features of the GLS formulation.

Keywords: Oldroyd-B model, Galerkin Least-Squares method, flow over a slot, viscoelastic inertial flows.

NOMENCLATURE

D	strain rate tensor (s^{-1})
f	bofy force (N)
H	channel height (m)
L_c	Characteristic length (m)
N_1	First normal stress difference (Pa)
p	hydrostatic pressure (Pa)
$\mathbf{Re}_r$	Rheological Reynolds number
u	velocity vector (m/s)
x	coordinate vector (m)
Wi	Weissenberg number

Greek symbols

α	stability parameter for momentum equation
β	stability parameter for the material equation
δ	stability parameter for continuity equation
$\dot{\gamma}$	strain rate, s^{-1}
λ	relaxation time (s)
ρ	density, kg/m^3
τ	extra-stress magnitude (Pa)
$\boldsymbol{\tau}$	extra-stress tensor (Pa)
μ	viscosity (Pa.s)

Subscripts

s	solvent
p	polymeric

Superscripts

*	dimensionless variables

INTRODUCTION

Numerical methodologies are an important tool to study fluid flows involving complex fluids, since experiments with those materials can be very expensive and time consuming. In the last three decades, lots of effort have been done on the development of accurate methods to analyze flows of viscoelastic fluids through complex geometries employing different constitutive equations and benchmark problems. However, difficulties to achieve convergence for highly elastic fluids still occur, and the problem continues under investigation in the literature.

The present article performs multi-field Galerkin least-squares (GLS) approximations in terms of extra-stress, pressure and velocity fields, for non-linear differential viscoelastic flows. The selected model is the upper-convected Oldroyd model, namely the Oldroyd-B model. This GLS methodology – introduced by Hughes et al. (1986) for the Stokes problem, was later extended to mixed Navier-Stokes equations in Franca and Frey (1992) and multi-field Navier-Stokes equations in Behr et al. (1993). It does not need to satisfy the compatibility conditions arisen from finite element sub-spaces for

the pair pressure–velocity – known as Babuška-Brezzi condition – and for the pair extra-stress–velocity. This is accomplished by adding mesh-dependent terms, which are functions of residuals of the flow governing equations, evaluated element-wise. In this way, both conditions may be circumvented and the methodology still remains stable – employing simple combinations of equal-order finite element interpolations – even for locally elastic-dominated flows, in which the upper-convected derivative of the extra-stress tensor plays a relevant role.

The Oldroyd-B model may accommodate both the Newtonian and upper-convected Maxwell models, covering the cases where an elastic fluid described by the Maxwell relation is mixed with a fluid governed by the Newton's law of viscosity – it corresponds to a situation in which an elastic polymer with a given viscosity is dissolved in a viscous solvent with different viscosity. The Maxwell fluid presents some difficulties on numerical simulations, partially because of the convective character of the stress evolution equation. With the small addition of a Newtonian solvent in the Oldroyd-B fluid model, the issue associated with the discretization of advective systems is strongly minimized.

The numerical solution of steady flows of Oldroyd-B fluids over a square slot is obtained and compared with some results from the literature. The geometry and the viscosity ratio are held fixed. The elastic effects are evaluated for a Weissenberg number range from 0 to 0.3; the inertia effects are evaluated for a rheological Reynolds number range from 0 to 75. All numerical results proved to be physically meaningful, and in accordance with the related literature.

MECHANICAL MODELING

Let Ω be the fluid domain, an open bounded subset of $\Re^2$ with a regular polygonal boundary Γ. A multi-field boundary-value problem for steady flows of Oldroyd-B fluids may be formed coupling the upper-convected Maxwell viscoelastic equation with the continuity and momentum equations – adding to the last a diffusive term to accommodate the effects of the addition of a Newtonian solvent (Behr et al., 2004) – subjected to appropriate velocity and stress boundary conditions:

$$\begin{aligned}
&\rho(\nabla \mathrm{u})\mathrm{u} = \nabla\cdot\boldsymbol{\tau} + 2\mu_s\nabla\cdot\mathrm{D}(\mathrm{u}) - \nabla p + \mathrm{f} && \text{in } \Omega\\
&\boldsymbol{\tau} + \lambda\overset{\nabla}{\boldsymbol{\tau}} = 2\mu_p\,\mathrm{D}(\mathrm{u}) && \text{in } \Omega\\
&\nabla\cdot\mathrm{u} = 0 && \text{in } \Omega\\
&\mathrm{u} = \mathrm{u}_g && \text{on } \Gamma_g^{\mathrm{u}}\\
&\boldsymbol{\tau} = \boldsymbol{\tau}_g && \text{on } \Gamma_g^{\tau}\\
&\left[\boldsymbol{\tau} - p1\right]\mathrm{n} = \mathrm{t}_h && \text{on } \Gamma_g
\end{aligned} \tag{1}$$

where **u** is the velocity vector, p is the hydrostatic pressure, and $\boldsymbol{\tau}$ is the extra-stress tensor – the primal variables of the problem; ρ is the fluid density, λ is the fluid relaxation time, μ_s and μ_p are, respectively, the solvent and the polymeric viscosity, **D** is the strain rate tensor, **f** is the body force, $\boldsymbol{\tau}_h$ is the stress vector, $\mathbf{u}_g$ and $\boldsymbol{\tau}_g$ are the imposed velocity and extra-stress boundary conditions, respectively, and $\overset{\nabla}{\boldsymbol{\tau}}$ stands for the upper-convected time derivative of $\boldsymbol{\tau}$:

$$\overset{\nabla}{\boldsymbol{\tau}} = (\nabla\boldsymbol{\tau})\mathrm{u} - (\nabla\mathrm{u})\boldsymbol{\tau} - \boldsymbol{\tau}(\nabla\mathrm{u}^T) \tag{2}$$

In order to obtain the dimensionless governing parameters, the rheological normalization introduced by de Souza Mendes (2007) is applied. Therefore, the following set of dimensionless quantities are introduced:

$$\begin{aligned}
&\mathrm{x}^* = \frac{\mathrm{x}}{L_c};\ \mathrm{u}^* = \frac{\mathrm{u}}{\dot\gamma_c L_c};\ p^* = \frac{p}{L_c};\ \boldsymbol{\tau} = \frac{\boldsymbol{\tau}}{\mu_t\dot\gamma_c};\\
&\mu_p^* = \frac{\mu_p}{\mu_t};\ \mu_s^* = \frac{\mu_s}{\mu_t};\ \mathrm{f}^* = \frac{\mathrm{f}}{\mu_t\dot\gamma_c / L_c}
\end{aligned} \tag{3}$$

where $\dot\gamma_c$ is the characteristic strain rate of the flow, and L_c is the characteristic length – in this work taken equal to $1/\lambda$ and H (the main channel height, see Fig. 1), respectively – and $\mu_t = \mu_p + \mu_s$.

Hence, substituting the dimensionless variables introduced above into the boundary value problem given by Eq. (1), the dimensionless multi-field formulation for inertia flows of Oldroyd-B fluids is given by:

$$\begin{aligned}
&\mathrm{Re}_r\left(\nabla^*\mathrm{u}^*\right)\mathrm{u}^* - \nabla^*\cdot\boldsymbol{\tau}^\bullet - 2\mu_s^*\nabla^*\cdot\mathrm{D}^*\left(\mathrm{u}^*\right) + \nabla^* p^* = \mathrm{f}^* && \text{in } \Omega^*\\
&\boldsymbol{\tau}^\bullet + \boldsymbol{\tau}^\bullet = 2\mu_p^*\,\mathrm{D}^*\left(\mathrm{u}^*\right) && \text{in } \Omega^*\\
&\nabla^*\cdot\mathrm{u}^* = 0 && \text{in } \Omega^*\\
&\mathrm{U}^* = \frac{\mathrm{u}_g}{\left|\mathrm{u}_g\right|}\,\mathrm{Wi} && \text{on } \Gamma_g^{\mathrm{u}}\\
&\boldsymbol{\tau}^\bullet = \boldsymbol{\tau}_g^\bullet && \text{on } \Gamma_g^{\tau}\\
&\left[\boldsymbol{\tau}^\bullet - p^*1\right]\mathrm{n} = \mathrm{t}_h^* && \text{on } \Gamma_g
\end{aligned} \tag{4}$$

where $\left|\mathbf{u}_g\right|$ is the average of the modulus of the velocity vector $\mathbf{u}_g$ at the channel inlet, and $\mathbf{Re}_r$ is the rheological version for the Reynolds number, defined as

$$\mathrm{Re}_r = \frac{\rho\left(\dot\gamma_c L_c\right)L_c}{\mu_t} = \frac{\rho}{\mu_t\lambda L_c^{-2}} \tag{5}$$

The Weissenberg number, defined as the ratio between the fluid relaxation time and the flow

characteristic time, appears in the inlet boundary condition and is computed as

$$Wi = \frac{\lambda}{L_c \left|\bar{\mathrm{u}}_g\right|} \tag{6}$$

For Oldroyd-B fluid flows, the Reynolds number usually employed in the literature is related to the rheological Reynolds number by $\mathbf{Re}=\mathbf{Re}_r\, Wi$.

Remark: The rheological Reynolds number defined by Eq. (5) is a dimensionless group based only on the rheological fluid properties, and, therefore, entirely uncoupled from the flow kinematics. De Souza Mendes (2007) suggests this definition claiming that $\mathbf{Re}_r$ may be viewed as a dimensionless fluid density.

THE FINITE ELEMENT APPROXIMATION

Based on usual definitions of finite element sub-spaces for extra-stress (Σ^h), pressure (P^h) and velocity ($\mathbf{V}^h$) (see, for instance Behr et al. 1993), a multi-field GLS formulation for Oldroyd-B fluid flows may be written as: Find the triple

$$\left(\boldsymbol{\tau}^h, p^h, \mathbf{u}^h ; \mathbf{S}^h, q^h, \mathbf{v}^h\right) \in \boldsymbol{\Sigma}^h \times P^h \times \mathbf{V}^h$$

such that

$$\begin{aligned}
&\int \rho \nabla\left(\mathrm{u}^h\right)\mathrm{u}^h \cdot \mathrm{v}^h \, d\Omega + \int \boldsymbol{\tau}^h \cdot \mathrm{D}\left(\mathrm{v}^h\right) d\Omega + 2\mu_s \int \mathrm{D}\left(\mathrm{u}^h\right) \cdot \mathrm{D}\left(\mathrm{v}^h\right) d\Omega \\
&\quad - \int p^h \nabla \cdot \mathrm{v}^h \, d\Omega + \left(2\mu_p\right)^{-1} \int \boldsymbol{\tau}^h \cdot \mathrm{S}^h \, d\Omega + \\
&\left(2\mu_p\right)^{-1} \int \lambda \left(\left[\nabla \boldsymbol{\tau}^h\right]\mathrm{u}^h - \left[\nabla \mathrm{u}^h\right]\boldsymbol{\tau}^h - \boldsymbol{\tau}^h \left[\nabla \mathrm{u}^h\right]^T \right) \cdot \mathrm{S}^h \, d\Omega - \int \mathrm{D}\left(\mathrm{u}^h\right) \cdot \mathrm{S}^h \, d\Omega \\
&\quad + \int \nabla \cdot \mathrm{u}^h \, q^h d\Omega + \varepsilon \int p^h q^h d\Omega + \delta \int \nabla \cdot \mathrm{u}^h \nabla \cdot \mathrm{v}^h \, d\Omega \\
&\quad + \sum_{K \in \Omega^h} \int \left(\rho \nabla\left(\mathrm{u}^h\right)\mathrm{u}^h + \nabla p^h - \nabla \cdot \boldsymbol{\tau}^h - 2\mu_s \nabla \cdot \mathrm{D}\left(\mathrm{u}^h\right) \right) \cdot \\
&\quad \cdot \alpha\left(\mathrm{Re}_{r_K}\right) \left(\rho \nabla\left(\mathrm{v}^h\right)\mathrm{u}^h + \nabla q^h - \nabla \cdot \mathrm{S}^h - 2\mu_s \nabla \cdot \mathrm{D}\left(\mathrm{v}^h\right) \right) d\Omega \\
&+ 2\mu_p \beta \int \left(\left(2\mu_p\right)^{-1} \left(\boldsymbol{\tau}^h + \lambda \left(\left[\nabla \boldsymbol{\tau}^h\right]\mathrm{u}^h - \left[\nabla \mathrm{u}^h\right]\boldsymbol{\tau}^h - \boldsymbol{\tau}^h \left[\nabla \mathrm{u}^h\right]^T \right) - \mathrm{D}\left(\mathrm{u}^h\right) \right) \right. \\
&\left. \cdot \left(\left(2\mu_p\right)^{-1} \left(\mathrm{S}^h + \lambda \left(\left[\nabla \mathrm{S}^h\right]\mathrm{u}^h - \left[\nabla \mathrm{u}^h\right]\mathrm{S}^h - \mathrm{S}^h \left[\nabla \mathrm{u}^h\right]^T \right) - \mathrm{D}\left(\mathrm{v}^h\right) \right) \right) d\Omega \\
&= \int \mathrm{f} \cdot \mathrm{v}^h \, d\Omega + \int \mathrm{t}_h \cdot \mathrm{v}^h \, d\Gamma + \\
&\sum_{K \in \Omega^h} \int \mathrm{f} \cdot \left(\alpha\left(\mathrm{Re}_{r_K}\right) \left(\rho\left(\nabla \mathrm{v}^h\right)\mathrm{v}^h + \nabla q^h - \nabla \cdot \mathrm{S}^h - 2\mu_s \nabla \cdot \mathrm{D}\left(\mathrm{v}^h\right) \right) \right) d\Omega
\end{aligned} \tag{7}$$

where $\mathbf{Re}_{rk}$ denotes the grid rheological Reynolds number; $\alpha(\mathbf{Re}_{rk})$, β and δ are the stability parameters for the motion, material and continuity equations, respectively – see Franca and Frey (1992) and Behr et al. (1993) for their definitions.

NUMERICAL RESULTS

The multi-field GLS approximation for Oldroyd-B fluids (Eq. 7) is employed to simulate the flow over a one-to-one slot. Fig. 1 shows the geometry and a blown-up view of the employed mesh in the vicinity of the slot. The geometry is very similar to the ones used by Trogdon and Joseph (1982) and Mitsoulis et al. (2006). After a mesh independence test procedure, based on an acceptable error of 2% of the stress modulus value on the channel wall, the computational domain W^h is partitioned by 3,200 equal-order Lagrangian bi-linear (Q1) finite elements, rendering a total of 19,200 degrees-of-freedom. The smallest dimensionless mesh size, $h_{K\,\min}^{*}=h_K/H$, is equal to 0.071.

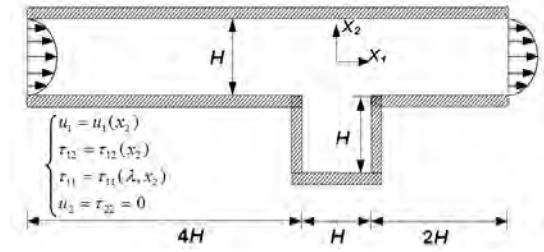

(a)

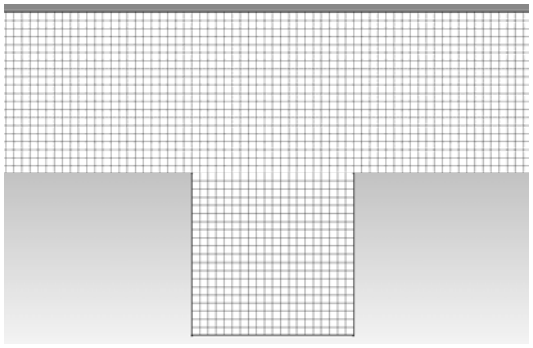

(b)

Figure 1. Flow over a slot: (a) problem statement; (b) a mesh detail.

The boundary conditions employed are impermeability and non-slip both on channel and on slot walls and viscoelastic fully-developed profiles for velocity and stress at the inflow and outflow of the channel. In addition, the relation between the solvent and total viscosities is held fixed - the chosen value used is in accordance with the related literature:

$$\frac{\mu_s}{\mu_s + \mu_p} = 0.59 \tag{8}$$

Figures 2 and 3 show the isobands for the dimensionless extra-stress τ_{11}^* and the first normal stress difference $N_1^* = \tau_{11}^* - \tau_{22}^*$, for creeping flows ($\mathbf{Re}_r$=0) and the Weissenberg number ranging from 0 to 0.3. It can be observed in Fig. 2 that τ_{11}^* is symmetric for the Newtonian fluid – Wi=0 (Fig. 2a) – in accordance with the inelastic fluid theory. When the Weissenberg number is increased, the Newtonian symmetry is broken, with the maximum value of τ_{11}^* occurring at the downstream corner of the slot, being

approximately eight times the maximum Newtonian peak (see Figs. 2a and 2b). The asymmetry presented by the viscoelastic τ_{11}^* component is surely credited to increasing of the fluid elasticity induced by the growth of the Weissenberg number. In Fig. 3a, for Wi=0, the first normal stress difference N_1^* is zero throughout the flow – the non-zero values of N_1^* found in the figure are due to the singularity introduced by the sharp shape of the slot corners. The null field for N_1^* is expected, since the Newtonian model is unable to prescribe non-null N_1^* values for shear flows. For the viscoelastic case (Wi=0.3), a gradient of the first normal stress difference N_1^* can be noticed near the channel walls and around the slot corners. Near the walls, boundary layers can be noticed and, around the channel centerline, a (flat) region of very small values for N_1^* is obtained. The appearance of boundary layers near the walls shows that, for viscoelastic flows, there is the up rise of a local vertical force – proportional to the first normal stress difference – acting on both walls of the channel.

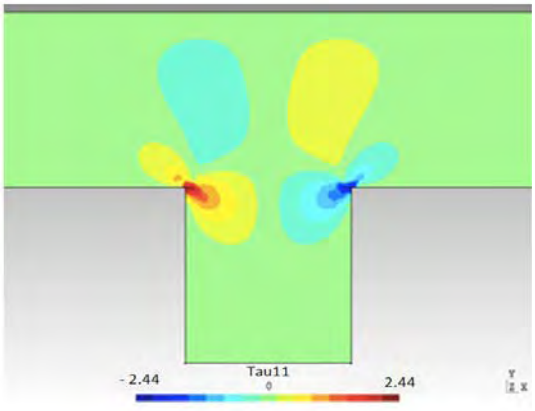

(a)

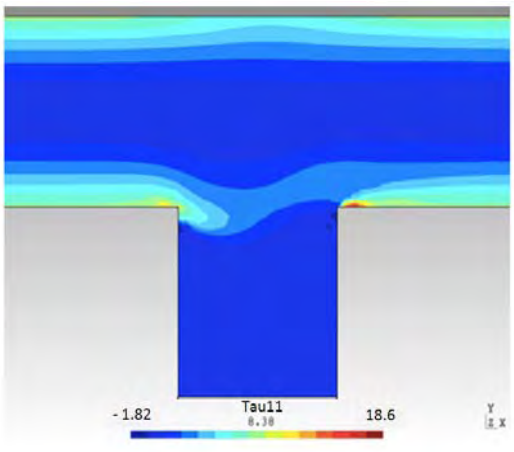

(b)

Figure 2. τ_{11}^* isobands for creeping flows: (a) Wi=0; (b) Wi=0.3.

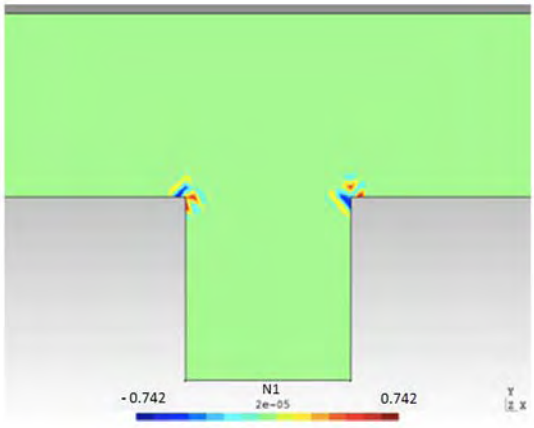

(a)

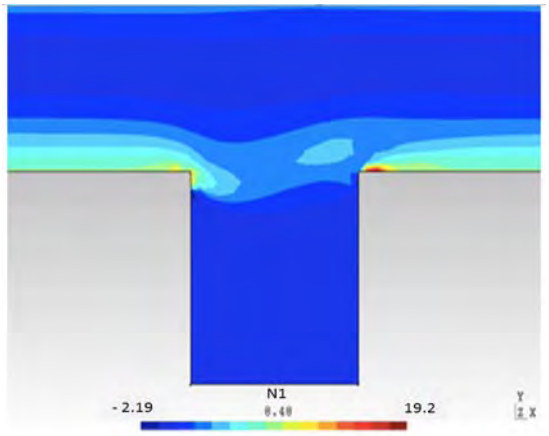

(b)

Figure 3. First normal stress difference N_1^* for creeping flows: (a) Wi=0; (b) Wi=0.3.

The results for inertial flows of Oldroyd-B fluids are shown in Figs. 4-7. Figs. 4 and 5 show an increase of the extra-stress values acting on the downstream corner of the slot, certainly due to the increase of momentum upwind through the channel. For the horizontal (u_1^*) and vertical (u_2^*) velocity fields (Figs. 6 and 7), the increase of the rheological Reynolds number produces an effect similar to that produced by increasing the Weissenberg number for non-inertial flows, that is to say, the larger the Reynolds number, the greater the asymmetry of the velocity fields. It is worth mentioning that the asymmetry presented by Figs. 2-3 is produced by the upwind effect of the upper-convected derivative of the extra-stress tensor of Eq. (2), since the rheological Reynolds number is equal to zero for those figures. On the other hand, the asymmetry of the inertia flows illustrated in Figs. 4-7 is generated by the mixed upwind behavior from the inertia term of the equation of motion and from the elastic term of the Oldroyd-B constitutive equation. Increasing the amount of inertia in the upper channel shifts the vortex inside the slot to the right, thus creating greater horizontal and vertical velocities on the vicinity of its right wall.

Finally, it is important to emphasize that the rheological dimensionless quantities defined by Eqs. (3)-(6) have fundamental importance on the investigation of the effects of inertia and elasticity on the flow. Thanks to this new methodology, the amount of inertia on the flow can be increased without changing the level of the fluid elasticity, or more specifically, in Figs. 4-7 it is possible to increase the rheological Reynolds number and hold the fluid properties fixed, for the same Weissenberg number.

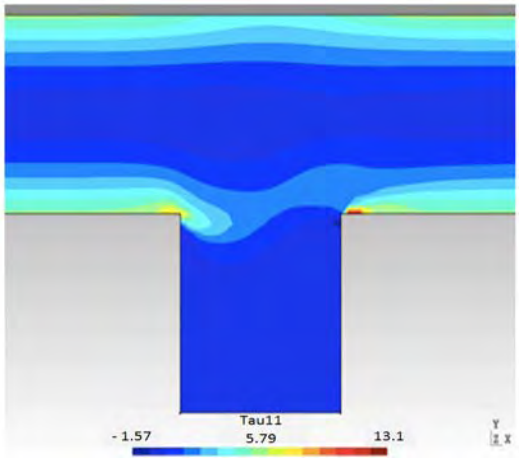

(a)

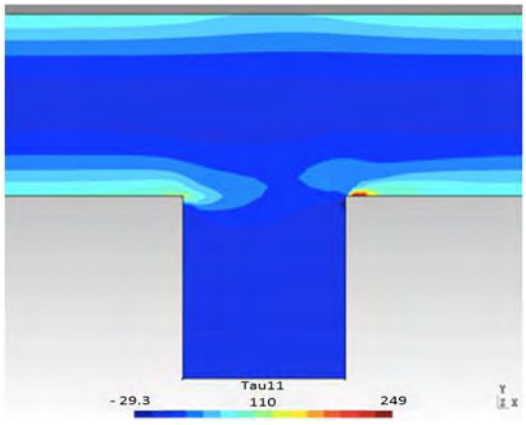

(b)

Figure 4. τ_{11}^{*} isobands for *Wi*=0.2: (a) Re_r=5; (b) Re_r=75.

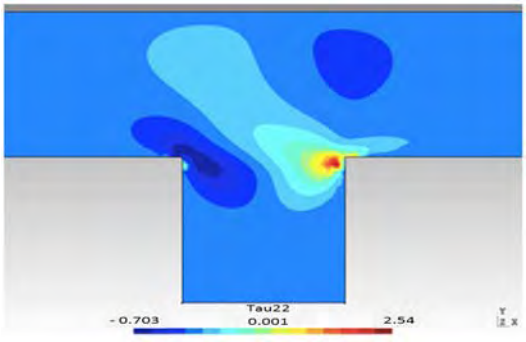

(a)

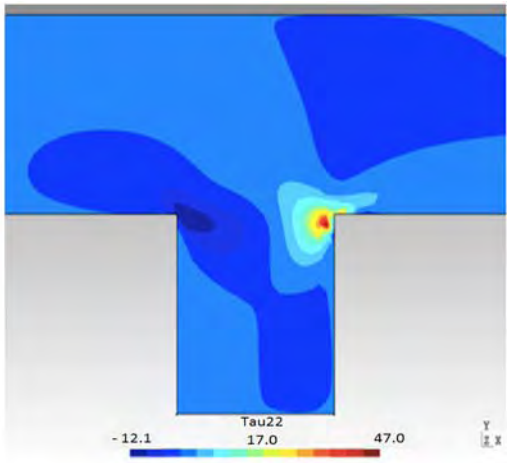

(b)

Figure 5. τ_{11}^{*} isobands for *Wi*=0.2: (a) Re_r=5; (b) Re_r=75.

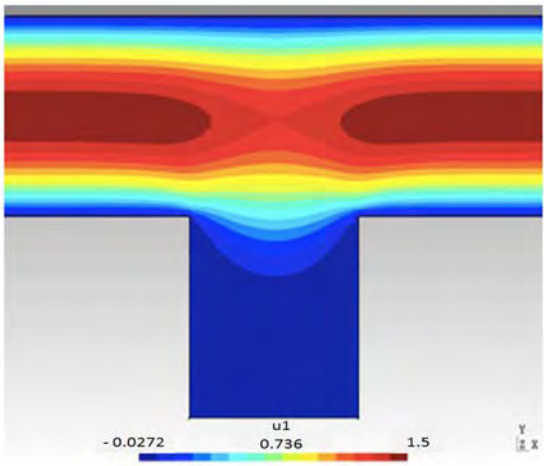

(a)

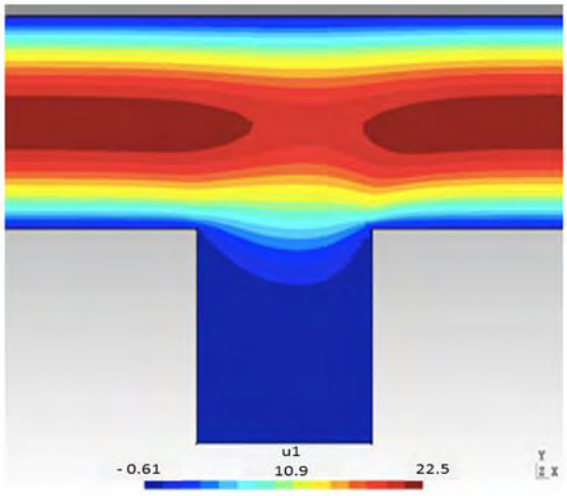

(b)

Figure 6. u_1^{*} isobands for *Wi*=0.2: (a) Re_r=5; (b) Re_r=75.

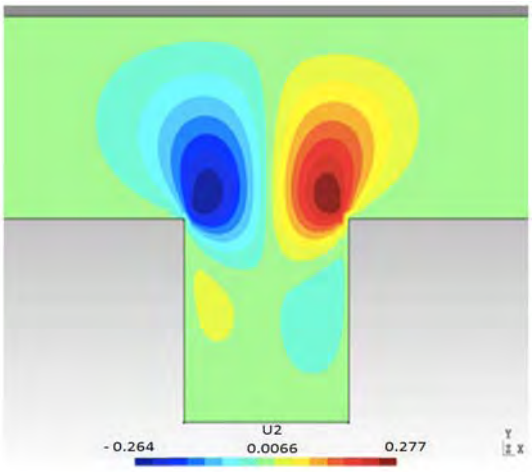

(a)

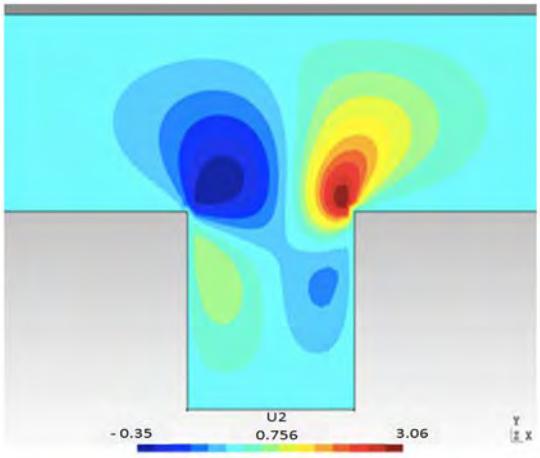

(b)

Figure 7. u_2^* isobands for Wi=0.2: (a) Re_r=5; (b) Re_r=75.

FINAL REMARKS

In this article, a multi-field GLS approximation for the Oldroyd-B constitutive model is introduced and discussed. Some numerical computations for inertia and inertialess flows through a channel over a slot are presented. The influence of inertia and fluid viscoelasticity on the velocity and stress fields were presented and analyzed, with the aid of a new definition of dimensionless rheological quantities. These are obtained following the definitions proposed in Souza Mendes (2007), which allows a better analysis of the effects of inertia and elasticity on the flow. The results obtained show that elasticity and inertia generate an increase of the asymmetry of the flow pattern. The results obtained for the first normal stress difference are in agreement with the literature – null for Newtonian fluids and increasing with elasticity.

ACKNOWLEDGEMENTS

The author D. Dall'Onder dos Santos thanks for his graduate scholarship provided by CAPES, and the authors S. Frey, M. Naccache and P. R. de Souza Mendes acknowledge CAPES and CNPq for financial support.

REFERENCES

Behr, M., Coronado, O. M., Arora, D., and Pasquali, M., 2004, Stabilized Finite Element Methods of GLS type for Oldroyd-B Viscoelastic Fluid, in: *European Congress on Computer Methods in Applied Sciences and Engineering - ECCOMAS 2004* Jyvaskyla, Finland.

Behr, M., Franca, L. P., and Tezduyar, T. E., 1993, Stabilized Finite Element Methods for the Velocity-Pressure-Stress Formulation of Incompressible Flows, Computer Methods in Applied Mechanics and Engineering, Vol. 104, pp. 31-48.

Mendes, P. R. de S., 2007, Dimensionless Non-Newtonian Fluid Mechanics, Journal Non-Newtonian Fluid Mechanics, Vol. 147, pp. 109-116.

Franca, L. P., and Frey, S., 1992, Stabilized Finite Element Methods: II. The Incompressible Navier-Stokes Equations, Computer Methods in Applied Mechanics and Engineering, Vol. 99, pp. 209-233.

Hughes, T. J. R., Franca, L. P., and Balestra, M., 1986, A New Finite Element Formulation for Computational Fluid Dynamics: V. Circumventing the Babuška-Brezzi Condition: A stable Petrov-Galerkin Formulation of the Stokes Problem Accomodating Equal-Order Interpolations, Computer Methods in Applied Mechanics and Engineering, Vol. 59, pp. 85-99.

Mitsoulis, E., Marangoudakis, S., Spyratos, M., Zisis, T., and Malamataris, N. A., 2006, Pressure-Driven Flows of Bingham Plastics over a Square Cavity, Journal of Fluids Engineering, Vol. 128, pp. 993-1003.

Trogdon, S. A., and Joseph, D. D., 1982, Matched Eigen Function Expansions for Slow Flow over a Slot, Journal Non-Newtonian Fluid Mechanics, Vol. 10, pp. 182-213.